Research Journal of Applied Sciences, Engineering and Technology 7(2): 303-310, 2014
DOI:10.19026/rjaset.7.255
ISSN: 2040-7459; e-ISSN: 2040-7467

Submitted: April 09, 2013 Accepted: April 22, 2013 Published: January 10, 2014

Research Article

HF Radar Signal Processing Based on Tomographic Imaging and CS Technique

Qiang Yang and Yixia Pan
Institute of Electronic Engineering Technology, Harbin Institute of Technology, Harbin, China

Abstract: This study presents the application of a spotlight-mode synthetic aperture radar (SAR) imaging technique to the problem of high probablity target detection in high frequency (HF) radar system, attempting to improve its spatial resolution. The effects of finite aperture on resolution, sampling constraints and reconstruction over a complete angular range of 360 degrees are discussed. A Convolution Back Projection (CBP) algorithm has been applied to image reconstruction. In order to solve the range limitation of aspect angle with one radar-carrying platform, we collect data over a larger azimuthal range by making multi-aspect observations. Each straight line is a sub aperture over which we can perform the CBP algorithm. When we demand higher resolution for stationary target, it will cause blur with longer data acquisition time. Thus the application of the traditional imaging algorithm is limited. Compressed Sensing (CS) has recently attracted much interest as it can reduce the number of samples without compromising the imaging quality. Within this motivation, we discuss the applicability of CS and present the application constraint for HF radar system.

Keywords: CBP, CS, HF radar, multi-aspect observations, spotlight-mode SAR imagin0067

INTRODUCTION

High resolution radar imaging is a typical goal in both commercial and military applications. HF radars, as introduced in Paduan and Libe (2013), are capable of mapping observation area to ranges approaching 200 km with a resolution of a few kilometers. Systems with higher spatial resolution are critical for understanding target information. Since spotlight-mode SAR (Jakowatz *et al*., 1996) has proved to be a very effective microwave imaging technique for high resolution ground mapping, remote sensing and surveillance applications, we apply spotlight-mode SAR imaging technique in HF radar system, attempting to solve this problem in this study.

In spotlight-mode SAR, the range resolution is related to and limited by the signal bandwidth. The cross range resolution is determined by the bandwidth generated by the relative motion between the radar and the target (Coetzee *et al*., 2006). It is well known that the electromagnetic scattering characteristics of the true target in HF radar are different from the ideal scattering point model in X-ray radar. That is to say, the reflectivity density of the ground patch is not only related with the target position, but also with the sampled frequencies and viewing angles. When we apply SAR approach in HF radar, this factor needs to be considered.

In this study, one of the most popular Computer-Aided Tomography (CAT) signal processing algorithms, the CBP algorithm has been applied to image reconstruction. The resolution achievable in tomographic imaging is determined by the resolution of the 1D range or cross range profiles provided by the radar projections (Munson *et al*., 1983).

Circular Synthetic Aperture Radar (CSAR) as comprehensively introduced in Mehrdad (1999) illuminates the target over a complete angular range of 360°. In this manner, the obtained spatial spectrum for the scene can be very wide. Consequently, the spatial resolution can be very high (Zhang *et al*., 2006). This approach provides valuable insight into the fundamental resolution limits possible in HF radar system.

In practical application, the scene to be mapped is observed in a limited range of aspect angle for spotlight-mode SAR with only one platform. Then the synthetic aperture length can be obtained is limited. Furthermore, it will affect the spatial resolution. When collecting data over a larger azimuthal range by making a few observations, it can largely improve the spatial resolution in HF radar system.

In HF radar imaging system, when conventional algorithm (CBP) is applied for image formation, target range and cross range resolutions are, respectively, determined by the bandwidth of the transmitted signal and the size of array (Ahmad *et al*., 2005). Higher resolution imaging demands wider bandwidth and larger array and subsequently requires more data to process. Furthermore, reducing the number of samples

Corresponding Author: Yixia Pan, Institute of Electronic Engineering Technology, Harbin Institute of Technology, Harbin, China

reduces the acquisition time and saves signal bandwidth. This reduction is important when surveillance is performed within small time window and when targets are required to remain stationary without translation or rotation motions, to avoid blurring and smearing of images. Clearly, it is impossible to see this promise in conventional algorithm.

Recently the area known as CS (Patel *et al*., 2010) has received much attention in the signal processing field. CS seeks to acquire as few measurements as possible about an unknown signal and given these measurements, reconstructs the signal either exactly or with provably small probability of error (Edmund and Frederick, 2009). In this study, we examine the implications of CS on HF radar reconstruction quality.

MONO-STATIC SPOTLIGHT-MODE SAR IMAGING

Mono-static spotlight-mode SAR is an example of high resolution radar imaging. In this case, an array aperture is required to provide cross range resolution. By processing a wideband signal that is transmitted and received at different spatial locations, a two dimensional high resolution image of the target or scene of interest can be obtained. Considering the different electromagnetic scattering characteristics of the true target in HF radar, we can use this imaging model in HF radar system.

We consider a two dimensional imaging system. Use (x, y) and (k_x, k_y) to identify the spatial and the spatial frequency domains respectively. For a spatial domain signal $f(x, y)$, its spatial Fourier transform is denoted by $F(k_x, k_y)$. Assume that there is a target area illuminated by a mono-static spotlight-mode SAR system, as shown in Fig. 1.

Here, the target area illuminated by the radar in range is within $[X_c\text{-}X_0, X_c+X_0]$, in cross range is within $[Y_c\text{-}Y_0, Y_c+Y_0]$. Let X_c be the range distance to the center of the target area, Y_c the cross range distance to the center of the target area in the spatial domain . The x coordinate is used to identify range and y specifies the cross range domain. Suppose the radar moves along the line x = 0 on the (x, y) plane. The radar makes a transmission and its corresponding reception at $(0, u)$ for $u \in (\text{-L}, \text{L})$ (synthesized aperture) on the (x, y) plane. Soumekh (1991) discussed the total recorded echoed signal model.

The resolution and the size of the scene are determined by the frequency bandwidth, frequency step and the length of the array. Once the size of the scene and the required resolutions are specified, parameters of the radar signal such as minimum frequency bandwidth, frequency step, total measurement angle and angular step size are automatically determined.

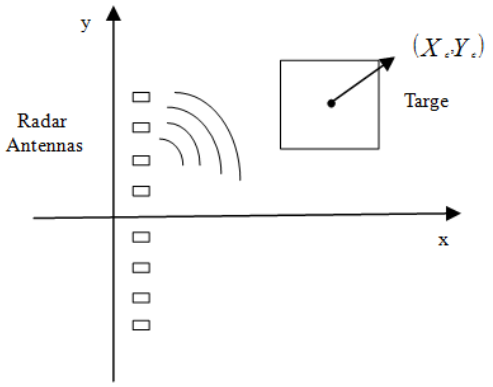

Fig. 1: Imaging geometry for mono-static SAR

Let B_x and B_y be the the bandwidth of f_x and f_y, respectively (Yeo-Sun and Amin, 2008):

$$B_x = f_N \cos\theta_M - f_0$$

$$B_y = 2f_0 \sin\theta_M \quad (1)$$

where,
f_0 = The minimum frequency
f_N = The maximum frequency
θ_M = The required antenna angle

Suppose that a D_x down-range resolution and D_y cross-range resolution image of $2X_0 \times 2Y_0$ sized scene is required. Then, the required frequency band width B_x is $c/2D_x$ and the required number of frequency bins n is $2X_0/D_x$. Furthermore, we can obtain the required frequency band width B_y ($B_y = 2Y_0/D_y$) and the required antenna angle θ_M.

Accordingly, the required synthesized aperture array length $2L$ is given by:

$$2L \approx 2X_{cc} \cdot \tan\theta_M \quad (2)$$

Where *Xcc* is the center of the scene away from the array for squint processing?

Similarly, the number of antenna position m_c is denoted by $2Y_0/D$. According to these specifications, the antenna should transmit and receive n narrow-band signals at m_c different positions.

m_c Projections are taken at equally spaced angles $\Delta\theta$, where $\Delta\theta$ is related to the maximum dimension D of the object (D = max($2X_0$, $2Y_0$) According to Mensa *et al*. (1983), this relationship is given by:

$$\Delta\theta \le \frac{\lambda}{2 \cdot D} \quad (3)$$

Let du_c 0062e the displacement between elements. Then one can obtain:

$$d_{u_c} \approx \Delta\theta \cdot X_{cc} \quad (4)$$

This means that the number and location of scatterers comprising the target will determine the number and distribution of apertures required to avoid grating lobes in the tomographic image.

SIMULATION AND ANALYSIS OF CSAR

CSAR can be regarded as a particular spotlight-mode SAR that its beam focuses on the target while the moving path of its platform is circular. The high spatial resolution is obtained by applying the principles of tomography to a HF radar system.

To examine this high resolution imaging concept, a multistatic CW radar geometry has been emulated using simulated data from point scatterers. The approach is based on well developed algorithms of tomographic processing to generate two dimensional high resolution imagery. Here, we assume the radar-carrying platform is ground-based. Consider an antenna forming a circular aperture with the target area at its centre. The configuration of the simulated system is that of chirp stepped-frequency HF radar viewing the area by 360degrees. Here, we construct a simple CSAR system model whose parameters are shown in Table 1.

Table 1: Parameters

Parameters	
RF carrier frequency	15 MHz
Baseband bandwidth	2 MHz
Number of elements	3218
Displacement between elements	97.65 m
Radius of target area	50 km
Pulse width	25 us
Target area in range	[50-2,50+2] km
Target area in cross-range	[0-2,0+2] km
Length of synthesized aperture	314 km

By sliding the aperture around in a circle, many projections may be formed which can be used to create a tomographic image, as shown in Fig. 2.

As is shown above, the resolution is limited to $\lambda/4$ in each dimention. Furthermore, Fig. 3 shows the backprojection reconstruction spectrum.

From the analyses above, we can see that the tomographic radar imaging algorithm can get the reflectivity function of the target and the resolution of the tomographic radar imaging algorithm is excellent for a HF radar system.

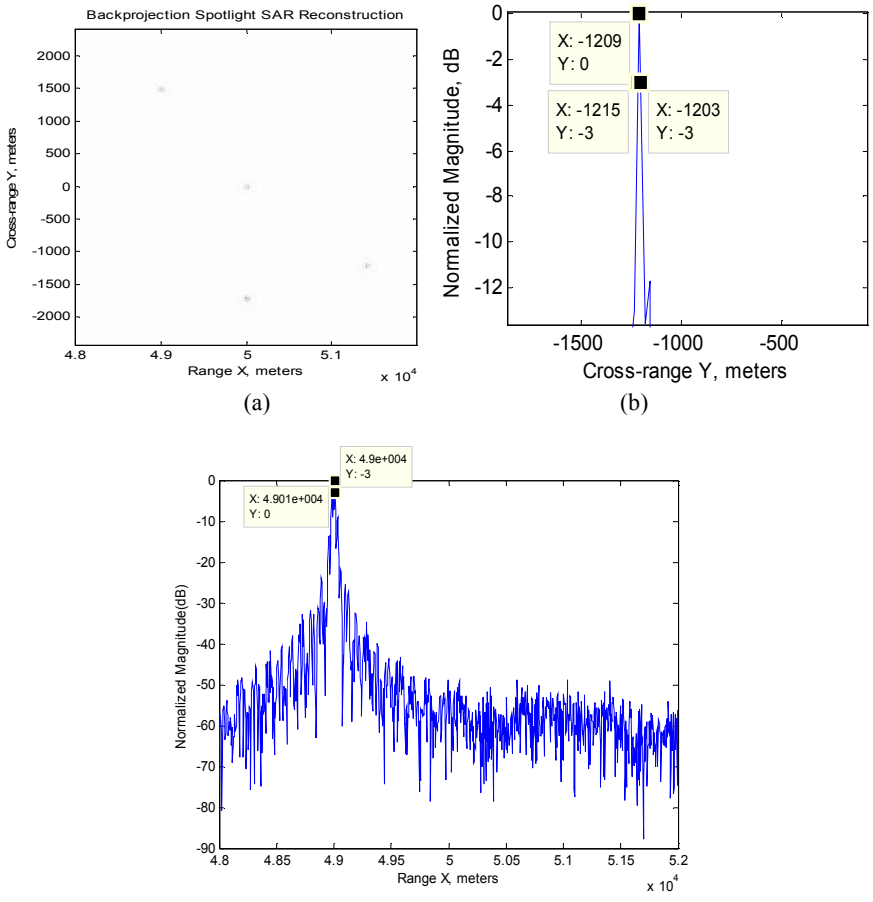

Fig. 2: A tomographic image formed from the backprojection reconstruction, (a) Images for four point targets, (b) Reconstruction in cross-range dimention for one target, (c) Reconstruction in range dimention for one target

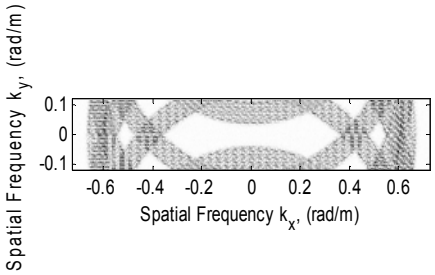

Fig. 3: Backprojection reconstruction spectrum

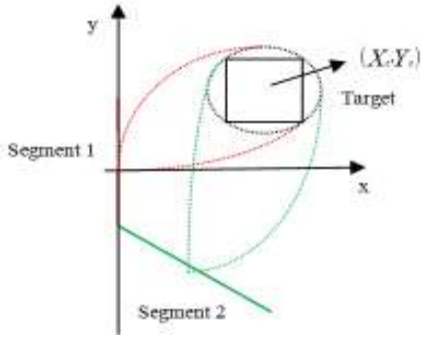

Fig. 4: Top view of two observations

It has been shown that the theoretical limitations on resolution in HF radar are determined by spatial sampling of the aperture rather than frequency sampling as in the case of SAR. Once the signal bandwidth is limited in practice, we can observe the same area through multiple aspects to obtain high reconstruction performance. This, in principle, provides us new approach to achieve higher resolution in HF radar system.

MULTI-ASPECT IMAGING OF HF RADAR

Traditionally, in spotlight-mode SAR, with the limitation of the radar itself characteristic, radar carrier and the trajectory of the platform (Zhang *et al*., 2007), the scene to be mapped is still observed in a limited range of aspect angle.

Here, we can collect data over a larger azimuthal range by making a few observations through different viewing angles. Each observation can be regarded as a spotlight-mode SAR that its beam focuses on the same target area while the moving path of its platform is a straight line. Each straight line is a subaperture over which we can perform the CBP algorithm. The separate spatial spectrum can be fused together to form a much

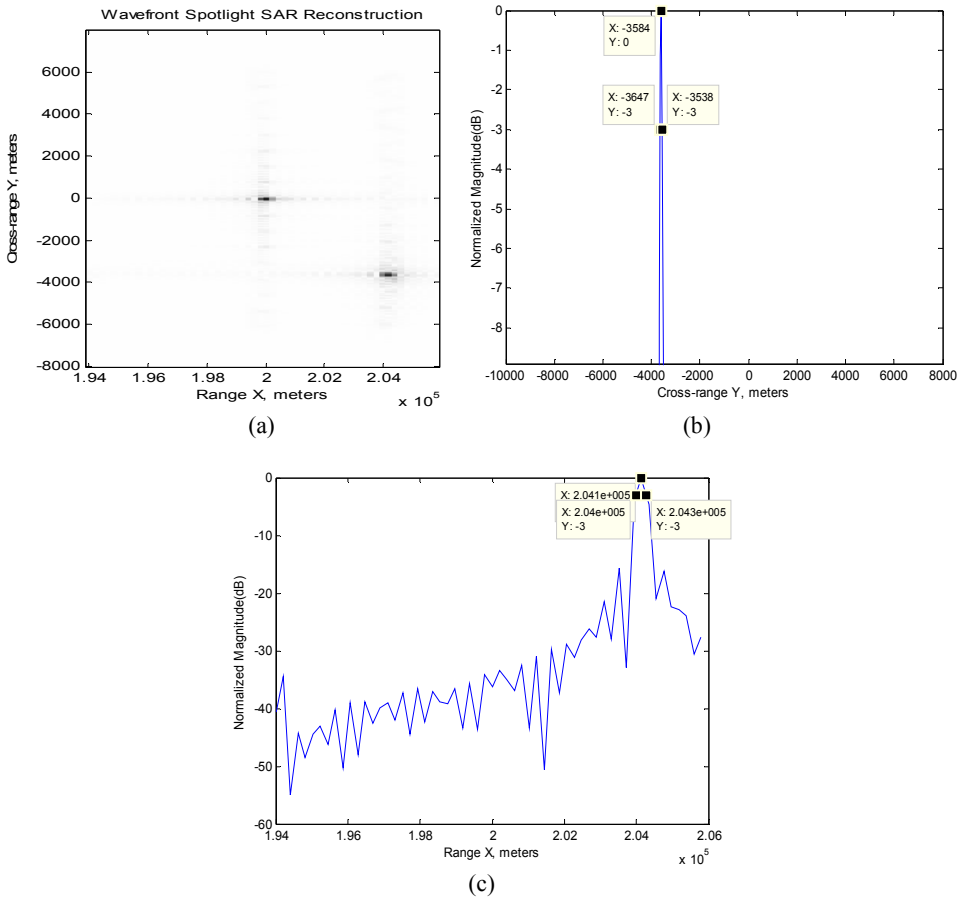

Fig. 5: Image formed from one observation, (a) Images for two point targets, (b) Reconstruction in cross-range dimention for one target, (c) Reconstruction in range dimention for one target

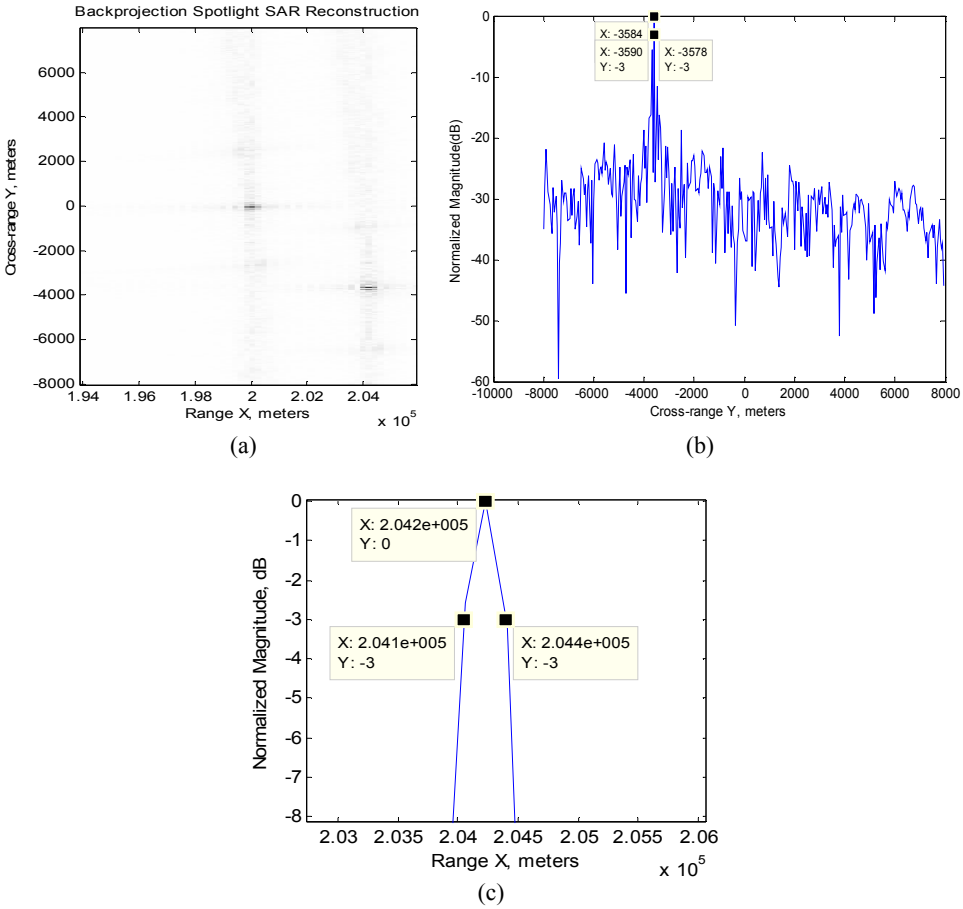

Fig. 6: Image formed from two observations, (a) Images for two point targets, (b) Reconstruction in cross-range dimention for one target, (c) Reconstruction in range dimention for one target

Table 2: Parameters

Parameters	
RF carrier frequency	15 MHz
Baseband bandwidth	200 KHz
Number of elements	88
Displacement between elements	138 m
Pulse width	2.5 us
Target area in range	[200-6,200+6] km
Target area in cross-range	[0-6,0+6] km
Length of synthesized aperture	16 km/16 km

wider one after processing all subapertures. Consequently, the spatial resolution can be largely improved.

In this study, we apply this approach to a HF radar system. Here, suppose the path is divided into two segments evenly as Fig. 4 shows. The simulation parameters are summarized in Table 2.

First, we consider one observation. For each aspect imging, after two steps of convolution and back projection, a projection was computed and performed to obtain an image due to this one projection, as shown in Fig. 5.

Then we adopt the same imaging algorithm for the second observation. As additional projections were recorded and filtered, the obtained spatial spectrum for the scene can be very wide. In this manner, the intensity contributions of these are added to the new formed image, as Fig. 6.

Contrast Fig. 5 and 6, we can obtain that as the contributions of more and more filtered projections are added, the target slowly improves in azimuth dimension. Furthermore, the performance of point target imaging only improves in cross-range resolution. Another improvement effect is that comprehensive observations also inhibit side lobe of the impulse response, avoiding blurring and smearing of image. In this way, it demonstrates that the method of multi-aspect observations is possible to be applied in HF radar system.

CS IN HF RADAR

Signal model: CS has recently attracted much interest because of its important offerings and versatility. The application is characterized by sparse imaging where targets of interest are few and have larger cross-section than clutter objects. It is noted that in HF radar

applications, the number of targets is very small compared to the number of pixels in the image.

This model applies the CS theory by constructing complete target information dictionary, estimating the reflection coefficients of all the locations. Furthermore, it overcomes scintillations of RCS and enhances system resolution and detection capability of weak target in HF radar (Zhou *et al*., 2011). In this study, we discuss applicability of CS to HF radar.

The reflectivity density of the ground patch is modeled by the complex function $f(x,y,\theta,\omega)$. It is assumed that the reflectivity density is variational over the range of frequencies and viewing angles employed by HF radar. Munson *et al*. (1983) discussed the return signal model after low-pass filtering, that is:

$$s_r(\theta,\tau)\approx\int_{-L}^{L} g_\theta(u,\tau)\exp\left\{-j\frac{4\pi}{c}\left[f_c+k_r\left(\tau-\frac{2r_0}{c}\right)\right]u\right\}du \quad (5)$$

where f_c is the carrier frequency and 2kr is the FM rate:

$$g_\theta(u_0,\tau)=\int_{-\infty}^{\infty} f(x,y,\theta,\tau)dv$$

$$=\int_{-\infty}^{\infty} f(u\cos\theta-v\sin\theta,u\sin\theta+v\cos\theta,\tau)dv \quad (6)$$

The (5) expression can be identified as the Fourier transform of the projection $g_\theta(u,\tau)$.

Application of CS: CS is a very effective technique to recover the original signal from a relatively small number of data samples.

Assume that the scene $f(q_x, q_y)$ can be converted into a very long vector by stacking its columns. That is:

$$f=\left[f_0^H\cdots f_{q_y-1}^H\right]^H \quad (7)$$

where,

$$f_n=\left[f[0,n]\cdots f[q_x-1,n]\right]^T \quad (8)$$

Similarly, let y be uniformly sampled data vector constructed by the same way"

$$y=\left[y_0^H\cdots y_{N\theta-1}^H\right]^H \quad (9)$$

where,

$$y_m=\left[y[0,m]\cdots y[N_f-1,m]\right]^T \quad (10)$$

The relation between y and f is given by:

$$y=\Psi f \quad (11)$$

where, Ψ is an $N_fN_\theta\times q_x.q_y$ matrix whose i,j th element is:

$$[\Psi]_{i,j}=\exp\left\{-j4\pi\frac{\left[2\pi f_c-2k_r\left(\tau_a-\frac{2r_0}{c}\right)\right]\cdot\left(x_c\cos\theta_b+y_d\sin\theta_b\right)}{c}\right\} \quad (12)$$

With

$$a=i\bmod N_f, b=\left[i/N_f\right], c=j\bmod q_x, d=\left[j/q_x\right], \quad (13)$$

where, [.] denotes the maximum integer that does not exceed the value.

In CS, we select only M samples from $N_fN_\theta\times q_x.q_y$ samples:

$$y_{cs}=\Phi\Psi f. \quad (14)$$

Randomly selected Fourier coefficients can be used as measurements that provide perfect image reconstruction with very high probability. In this case, the measurement matrix is a $M\times N_f.N_\theta$ matrix in which each row has only one non-zero element, equals to 1. The location of this unit value is randomly chosen.

EXPERIMENTAL RESULTS

We consider a mono-static HF Radar imaging systemasshown in Fig. 1 with a large ground patch of size ($2X_0$, $2Y_0$) (6, 6) km when observed over a narrow angle aspect cone of $\Delta\theta = 4.1$ deg.

The transmitted waveforms are chirp signals with f_c = 15MHz and B = 200 KHz. A nominal Rayleigh range resolution is $\rho_x = c/2B$ = 750 m and a nominal cross-range resolution is $\rho_y = \lambda/(4\sin(\Delta\theta/2))$ = 252 m The number of measurements is fixed to M = 400. In R and CS cases, the number of aspect angles N_θ and the number of chirp frequency samples N_f is varied such that $M = N_\theta$. N_f = 400 It also applies that the conventional grid of (N_θ, N_f) = (30, 92) points is down sampled uniformly at random to 400 points.

Assuming that a pixel spacing matches the Rayleigh resolution, we first seek to reconstruct a 2D image of the scene with 9×24 pixels in each dimension. Furthermore, we contrast CS reconstruction with the conventional CBP reconstruction with partial and complete data. The results are shown in Fig. 7.

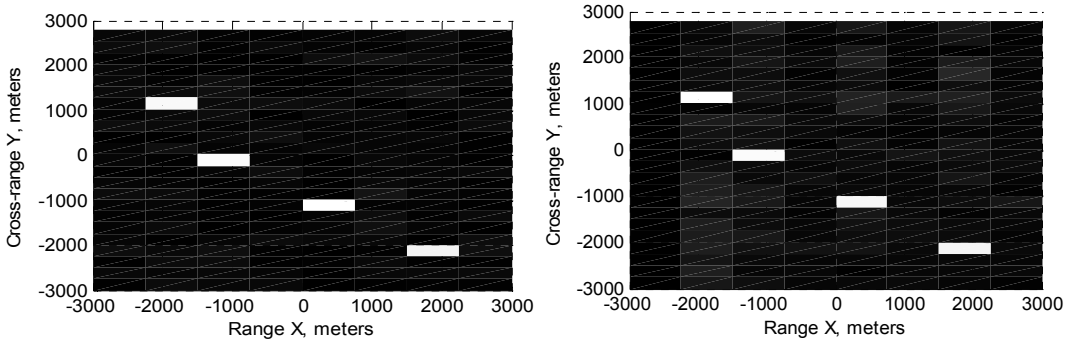

(a) (b)

Fig. 7: The pixel spacing matches the Rayleigh resolution, (a) Sparse reconstruction for RandCS case, (b) CBP reconstruction with complete data

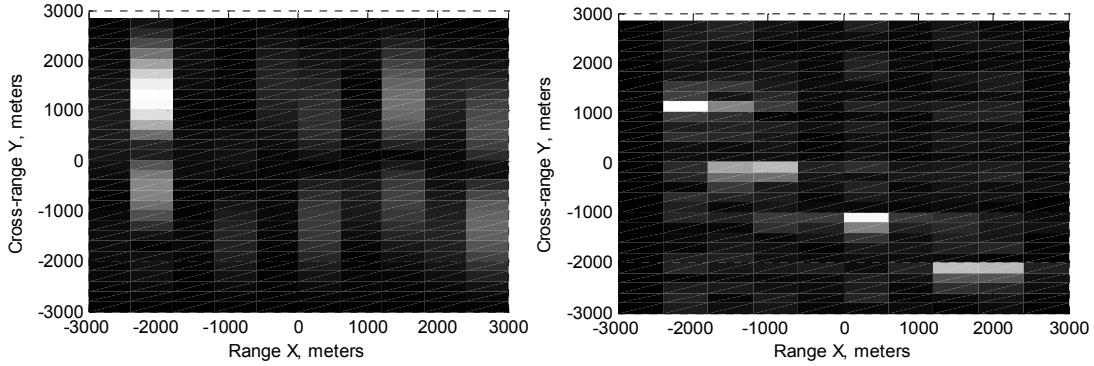

(a) (b)

Fig. 8: The pixel spacing is set to be smaller than its Rayleigh resolution, (a) Sparse reconstruction for RandCS case, (b) CBP reconstruction with complete data

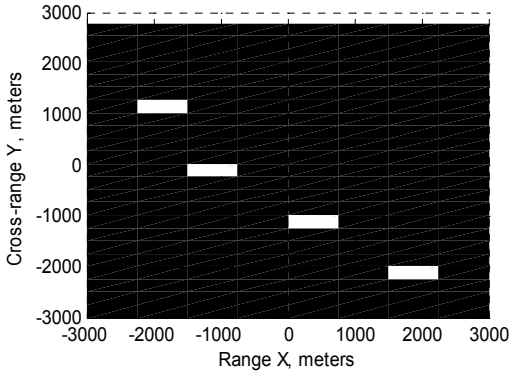

Fig. 9: Sparse reconstruction for RandCS case when the pixel spacing is set to be smaller than its Rayleigh resolution with constant reflectivity density

CBP reconstruction performs very poorly when few observations are available, but it can recover the scene with high quality by significantly increasing the number of measurements. As can be seen from the above results, CS using only 14% data needed for traditional algorithm can get almost equal image quality and resolution with CBP and better side lobe suppression performance.

When the pixel spacing is set to be (0.8*) ρ_x, 0.8*ρ_y) which is smaller than its Rayleigh resolution, some targets can take several pixels or part of some pixels, depending on their size and location in this case. Figure 8 show the reconstructed images, respectively.

As remarked earlier, the reflectivity density of the ground patch in HF radar is not only related with the target position, but also with the sampled frequencies and viewing angles. Note that the CS reconstruction performs very poorly in this case, as shown in Fig. 8a. Conversely, under the same conditions, when we use traditional CBP algorithm, it can still tell the four targets as shown in Fig. 8b, although there exits some sidelobe around target locations.

Furthermore, when we assume that the reflectivity density is constant over the range of frequencies and viewing angles, targets are clearly seen with lower side lobe level as Fig. 9 shows. In conclusion, CS has application constraints in HF radar system.

From above results, we can see that only when the pixel spacing is equal or greater than its Rayleigh resolution, CS can be effective in HF radar target

detection. The small number of data yields shorter data collection time, which is desired since targets should be stationary over the entire data collection.

CONCLUSION

Through analysis of literature and simulation results, we can obtain that the resolution and size of the image are limited by signal bandwidth, array length and frequency step and antenna displacement.

Simulations for CSAR imaging based on HF radar are presented to show that it can get much higher resolution in azimuthal direction than spotlight-mode SAR does with straight path. Furthermore, we propose an approach of multi-aspect imaging in HF radar system. As the contributions of more and more filtered projections are added, the target slowly improves in the azimuth dimension. When demanding higher resolution, CBP algorithm, as a means of traditional image reconstruction, is limited in practical application. Furthermore, we have demonstrated feasibility of CS techniques to solve this problem and give its corresponding application constraints in HF radar system.

REFERENCES

Ahmad, F., M. Amin and S. Kassam, 2005. Synthetic aperture beamformer for imaging through a dielectric wall. IEEE T. Aero. Elec. Sys., 41(1): 271-283.

Coetzee, S.L., C.J. Baker and H.D. Griffiths, 2006. Narrow band high resolution radar imaging. Proceeding of the IEEE Conference on Radar, pp: 622-625.

Edmund, G.Z. and D.G. Frederick, 2009. Compressed sensing of mono-static and multi-static SAR. Proceeding of SPIE 7337, Algorithms for Synthetic Aperture Radar Imagery XVI, 733705.

Jakowatz, C.V., T. Paul, E.W. Daniel, H.E. Paul and C.G. Dennis, 1996. Spotlight-Mode Synthetic Aperture Radar: A Signal Processing Approach. Kluwer Academic Publishers, Norwell.

Mehrdad, S., 1999. Synthetic Aperture Radar Signal Processing with MATLAB Algorithms. John Wiley and Sons, New York, pp: 648.

Mensa, D.L., S. Halevy and G. Wade, 1983. Coherent Doppler tomography for microwave imaging. Proc. IEEE, 71(2): 254-261.

Munson, D., J. O'Brien and W. Jenkins, 1983. A tomographic formulation of spotlight-mode synthetic aperture radar. Proc. IEEE, 71(8): 917-925.

Paduan, J.D. and W. Libe, 2013. High-frequency radar observations of ocean surface currents. Ann. Rev. Marine Sci., 5: 115-136.

Patel, V.M., G.R. Easley, D.M. Healy and R. Chellappa, 2010. Compressed synthetic aperture radar. IEEE J. Select. Top. Signal Process., 4: 244-254.

Soumekh, M., 1991. Bistatic synthetic aperture radar inversion with application in dynamic object imaging. IEEE T. Signal Proces., 39: 2044-2055.

Yeo-Sun, Y. and M.G. Amin, 2008. Compressed sensing technique for high-resolution radar imaging. Proceeding of the SPIE 6968, Signal Processing, Sensor Fusion and Target Recognition, 17: 69681A.

Zhang, X., Y. Zhang and J. Jiang, 2006. Circular SAR imaging approximated by spotlight processing. Proceeding of 7th International Symposium on Antennas, Propagation and EM Theory (ISAPE '06), pp: 1-4.

Zhang, X., Y. Zhang and J. Jiang, 2007. Multi-aspect imaging of spotlight synthetic aperture radar. Chinese J. Radio Sci., 22: 577-582.

Zhou, S., Q. Yang and W. Deng, 2011. Based on CS distributed multi-carrier MIMO HF radar signal processing. J. Inform. Comput. Sci., 8: 1967-1976.